

## Forensic Examination of Trace Intumescent Fire-Retardant Coating

Wen-Tung Lo<sup>1</sup>, M.S. ; Jin-Cherng Huang<sup>2</sup>, Ph.D. ; Hsien-Hui Meng<sup>3</sup>, Ph.D. ; Yu-Ting Hsiung<sup>3</sup>, M.S. ; Wei-Tun Chang<sup>3\*</sup>, Ph.D.

<sup>1</sup> Forensic Science Section, Miaoli County Police Bureau, Miaoli, Taiwan R.O.C.

<sup>2</sup> Department of Wood Based Materials and Design, National Chiayi University, Chiayi, Taiwan R.O.C.

<sup>3</sup> Department of Forensic Science, Central Police University, Taoyuan, Taiwan R.O.C.

Received: October 25, 2016; Accepted: November 30, 2016.

### Abstract

During the investigations concerning uses of fire-retardant coating for fire safety or criminal purposes, it is often hard to visually distinguish between common architectural coatings and fire-retardant coatings on-site. This study aims to investigate trace intumescent fire-retardant coatings before and after a fire using micro Fourier transform infrared microspectroscopy (Micro-FTIR) and scanning electron microscopy (SEM)/energy-dispersive X-ray spectroscopy (EDS). Ten different types of intumescent fire-retardant coatings out of six brands were painted on plywood for testing according to the application standards of the manufacturers. The surface flammability test adopted was in accordance with Chinese National standards (CNS-6532). The resulting data indicated that after surface flammability test, those fire retardant coating samples could be differentiated from common architectural coatings by certain absorption peaks in IR spectra although the apparent spectral patterns of the two types of coatings were mostly similar except for two clear coatings. The SEM/EDS approach was then used to analyze characteristic elements for further discrimination of the coatings with similar IR spectra. Thus, all the fire retardant coatings of different brands were essentially distinguishable from architectural coatings. As the second part of the study, efforts were made to estimate the mixing ratio of mixed fire retardant-architectural coatings, and develop a combined FTIR and SEM/EDS method to distinguish them. The results showed that the intumescence effects of these mixtures were insufficient and these mixtures left different degree of cracking on the wooden surface.

**Keywords:** Forensic science, Trace fire-retardant coating, Fourier transform infrared microspectroscopy (FTIR), Scanning electron microscopy/Energy-dispersive X-ray spectroscopy (SEM/EDS)

### Introduction

Fire-retardant coatings have the same appearance as common architectural coatings at room temperature, and it is often hard not only to visually distinguish them but also to perform quality inspection of fire-retardant coatings on-site. During the production of fire-retardant coatings, besides the assessment of basic performances like coating type, coating composition, coating thickness, and application work, such material properties and

operational conditions as limiting oxygen index, ignition temperature, ignition time, after-flame time, afterglow time, rate of mass loss, damaged condition of protected material, development of smoke, and toxicity of smoke should also be inspected. The high cost of fire-retardant coating due to complicated inspecting procedure has led to low-priced, unqualified coatings produced by dishonest businessmen. This study combined forensic techniques and existing protocols for trace fire-retardant coatings in order to determine if a fire-retardant coating

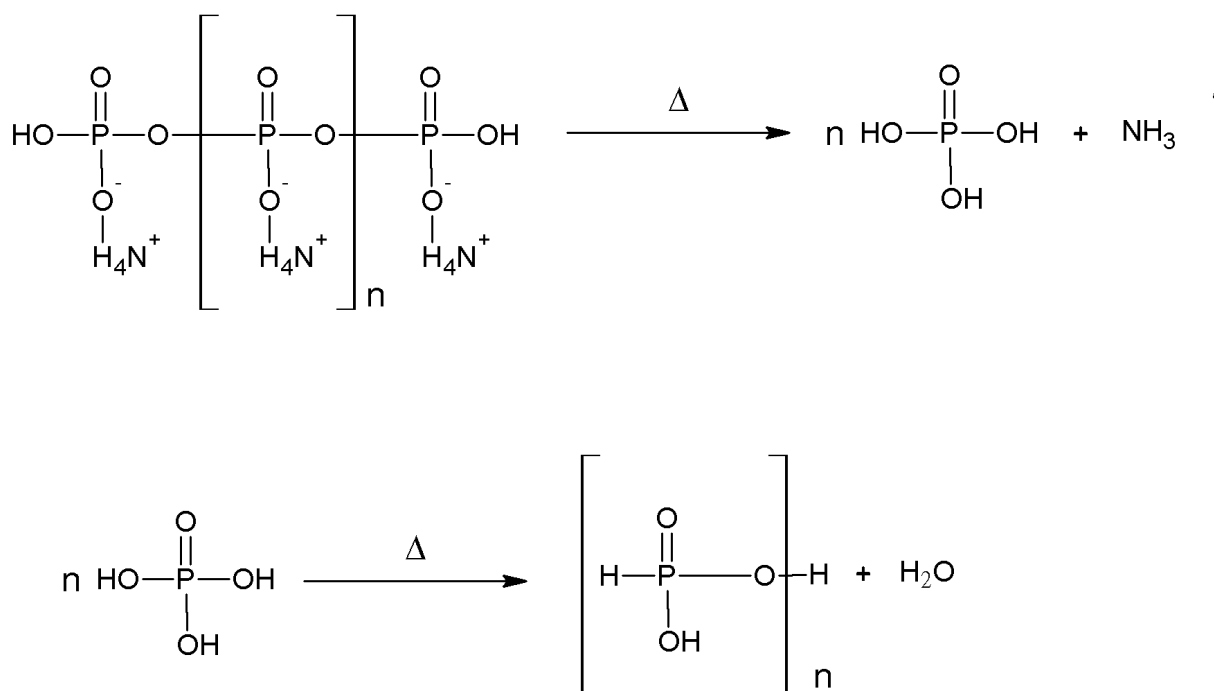
---

\*Corresponding author: Wei-Tun Chang, Department of Forensic Science, Central Police University, No. 56, Shuren Rd., Guishan Dist., Taoyuan City 33304, Taiwan, R.O.C.  
E-mail: una030@mail.cpu.edu.tw

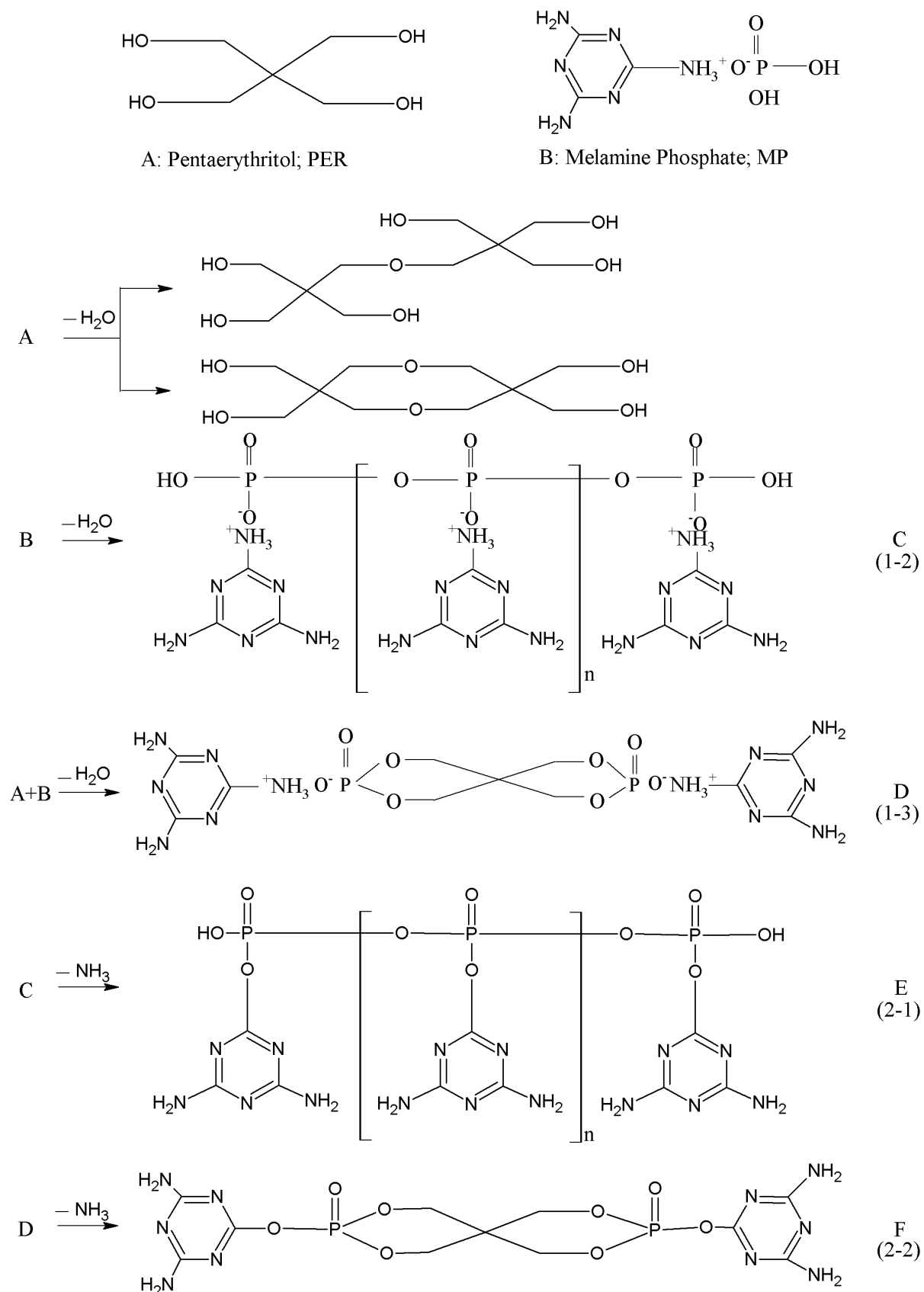
as a legal building material has been actually applied whenever it is required to be. That is, the proposed methods may serve as choices of protocols for fire safety inspection and fire investigation.

When exposed to heat, intumescent fire-retardant coatings will form a layer of foamed char with intumescent thickness expanded to 45–60 times the original thickness [1]. The materials include fire-retardant chemical, char former, foamer, vehicle, and fire-retardant filler. Conventional fire-retardant chemical is mainly composed of ammonium polyphosphate. Pentaerythritol and melamine are usually used as char former and foamer, respectively. Wang et al [2] and Lv et al [3] respectively studied thermal decomposition of ammonium polyphosphate and possible reactions

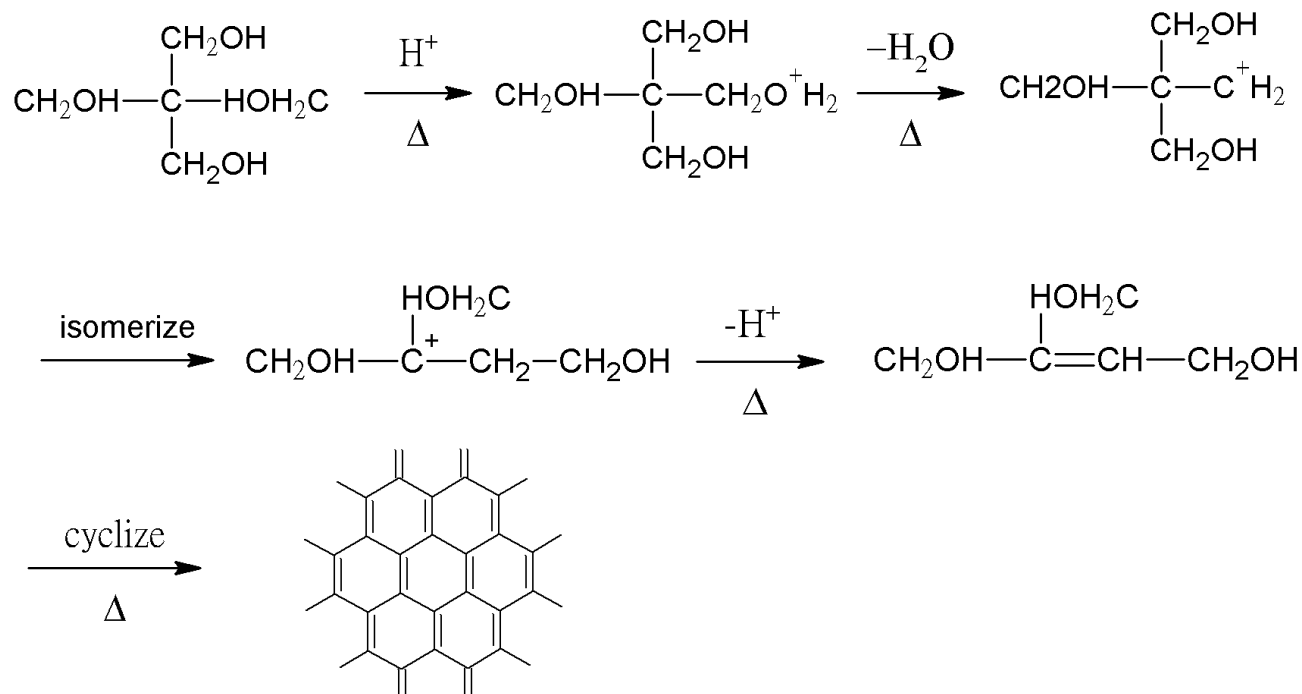
resulting from pentaerythritol/melamine phosphate composites under combustion. When heated, the fire retardant chemical generates phosphoric acid, ammonia, and water as shown in scheme 1 and scheme 2 respectively, where the phosphoric acid will catalyze a series of reactions of polyhydric alcohol producing water and alkene. The alkene proceeds to form a solid-phase char coating as shown in scheme 3. Meanwhile, the macromolecules of the underlying material depolymerize, leading to a decrease in melting temperature, and soften, shrink, and fuse into liquid below 250°C [4]. As a result, the air permeability of the char layer structure becomes extremely low and the underlying material is almost insulated from air, leading to fire retardation [5].



**Scheme 1** Thermal decomposition of ammonium polyphosphate [2].



**Scheme 2** Possible reactions resulting from pentaerythritol/melamine phosphate composites under combustion [3].



**Scheme 3** Reaction of char formation under combustion [2].

## Methods and Materials

### Standards and controls

Ten authentic samples of different types of intumescent fire-retardant coating from six brands as standards were collected from retailers in Taiwan. To prepare the controls of fire-retardant coating, each of the ten was painted on plywood with dimensions of 22 cm × 22 cm × 0.9 cm according to the coating standards of the manufacturer (Table 1).

### Mixed samples with varied volumes of fire retardant coatings

Two types of fire retardant coating used in this study, B-2 and C-3, were mixed respectively with an architectural coating (model G-1) manufactured by Company G. Specifically, B-2 and C-3 were each fully blended with G-1, with volume ratios of 1:2, 1:1, and 2:1. Each mixed coating was also painted on plywood.

### Fourier transform infrared microspectroscopy (micro-FTIR)

A Micro FT/IR-200 system (Jasco Inc., Japan)

assisted with a diamond compression cell (model DX1610E from Diamond EX'Press) was employed in this study. The measurement conditions were set as follows: range of wavenumber, 4000–650 cm<sup>-1</sup>; times of scans, 128. The specimen was processed under a microscope using scalpel blade #11 to scratch approximately 5 μg of sample at a low angle which was then placed on the diamond surface and compressed by two diamond pressing dies to form a thin flake suitable for infrared analysis.

### Scanning electron microscopy (SEM)/energy-dispersive X-ray spectroscopy (EDS)

A JOEL-JSM-5400/Link ISIS system with an accelerating voltage of 20 kV and magnification of ×750 (JEOL Ltd., Japan) was used to determine elemental data and their relative amounts. A 1-mm<sup>2</sup> sample was placed on a copper holder to conduct carbon coating by an SPI sputter coater.

### Surface flammability test

Surface flammability tests were conducted on specimens using a No. 239B Type II building material flammability tester (Yasuda Seiki Seisakusho Ltd., Japan). All specimens were placed in a chamber with

constant temperature (25 °C) and humidity (65%, RH) for a month. They were then dried in an oven at 35–40°C for 48 h and placed in a desiccator containing silica gel for at least 24 h. The Grade 3 fire resistance test was

then conducted in accordance with the method of test for incombustibility of interior finish material of buildings as described in CNS 6532 [6].

**Table 1** Different types of intumescent fire-retardant coatings and painting conditions.

Label	Type	Total wet coating	Dry film (mm)	Brush layer	Drying time (h)
A	A-1	0.23 L/m <sup>2</sup>	0.9	3	4-6
	A-2 <sup>a</sup>	0.21 L/m <sup>2</sup>	0.55	2	4-6
B	B-1	700 g/m <sup>2</sup>	0.5	2	24
	B-2	900 g/m <sup>2</sup>	0.6	3	24
	C-1 <sup>a</sup>	518 g/m <sup>2</sup>	0.35		24
C	C-2	910 g/m <sup>2</sup>	0.7	4	2
	C-3	910 g/m <sup>2</sup>	0.7	4	2
D	D-1	1000 g/m <sup>2</sup>	0.6		2-3
E	E-1	727 g/m <sup>2</sup>	0.33	3	3
F	F-1	800 g/m <sup>2</sup>	0.8	2-3	3-4

<sup>a</sup> A-2 and C-1 are clear paints, and the others are white paints.

**Table 2** Major absorptive bands for fire retardant coatings before and after combustion.

Wave number (cm <sup>-1</sup> )	Functional group
3400	O-H
3160	N-H
2960	C-H
2365	O=P-OH
1735	C=O
1680	P-OH
1635	C=C
1558	C-N (ring vibration)
1435	C-N (ring vibration)
1267	P=O-NH <sub>4</sub> (P=O, C-N)
1300~1150	P-O-C (complexes phosphate-carbon)
1135	C-O (P-O-C)
1089	P-O-P (P-O)
1020	P-O-P
895	N-H

## Results and Discussion

### *FT-IR microscopic analysis of fire-retardant coatings before and after combustion*

Generally, the IR spectra of fire-retardant coatings containing fire-retardant chemical, foamer, and char former displayed the following absorption bands: 3160 cm<sup>-1</sup> indicated the existence of an N-H functional group); 3324 cm<sup>-1</sup> corresponded to an O-H functional group; 1732 cm<sup>-1</sup> indicated a C=O functional group); 1673 cm<sup>-1</sup> represented a P-OH functional group [5]; 1438 cm<sup>-1</sup> indicated C-H and N-H functional groups; 1267 cm<sup>-1</sup> corresponded to phosphate (P=O); 1076 cm<sup>-1</sup> and 1016 cm<sup>-1</sup> both indicated the existence of a P-O-P functional group; 897 cm<sup>-1</sup> was the absorption peak of an N-H functional group. The details are tabulated in Table 2.

When the heating temperature increased, dehydration occurred in the hydroxy organophosphates or related polymers on the surface of a fire-retardant coating and produced more stable counterparts, which first appeared as a fused, viscous substance, and then began to decompose into phosphoric acid and  $\text{NH}_3$  at approximately  $250^\circ\text{C}$  while the intermediates of the dehydration reaction present in the middle layer between charred and uncharred layer, and phosphoric acid further dehydrates to form polyphosphate at above  $300^\circ\text{C}$  [2]. The generation of other  $\text{NH}_3$  in the intumescent fire-retardant coating from stage C and Stage D during combustion was shown in Scheme 2 [3]. In the absorption range of  $1300\text{--}900\text{ cm}^{-1}$  in the IR spectrum, the absorption band around  $1260\text{--}1250\text{ cm}^{-1}$  corresponded to the stretching of a  $\text{P}=\text{O}$  functional group. The absorption band around  $1300\text{--}1150\text{ cm}^{-1}$  represented the complex  $\text{P-O-C}$  group produced from phosphate (ester) and the carbon in pentaerythritol [7]. The absorption peak at  $1090\text{ cm}^{-1}$  corresponded to the vibration of a  $\text{P-O}$  group in a  $\text{P-O-P}$  linkage. After combustion, the absorption peaks around  $3324\text{--}3200\text{ cm}^{-1}$  were dampened and the peak at  $2350\text{ cm}^{-1}$  representing an  $\text{O}=\text{P-OH}$  group appeared. The absorption peak at  $1728\text{ cm}^{-1}$  corresponding to the carbonyl ( $\text{C}=\text{O}$ ) disappeared in the IR spectrum of char layer. The tiny absorption peak at around  $1640\text{ cm}^{-1}$  indicated the formation of a  $\text{C}=\text{C}$  bond [8]. The peak intensity at  $1412\text{ cm}^{-1}$  corresponding to  $\text{N-H}$  and  $\text{C-H}$  groups tended to decrease. The absorption peak of a  $\text{P-O-C}$  group appeared in the band around  $1100\text{--}1000\text{ cm}^{-1}$ , and that of the phosphate ( $\text{P}=\text{O}$ ) group appeared around  $1250\text{--}1200\text{ cm}^{-1}$ . The peak at  $1062\text{ cm}^{-1}$  represented a  $\text{P-O}$  group.

#### ***Discrimination between commonly used intumescent fire-retardant coatings***

The inspection of surfaces with different types of fire-retardant coatings via SEM ( $\times 750$ ) only showed distinct differences between the meadow-like shredded pattern of type A-1 and the plane flake pattern of other types of fire-retardant coatings (Fig. 1).

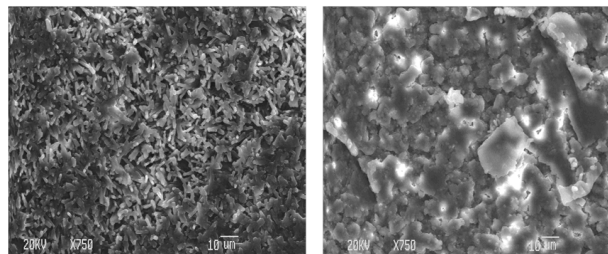


**Fig. 1** The surface appearance of Type A-1 (left) and B-1 (right) in the SEM ( $\times 750$ ).

FTIR methods proposed by Roger et al. [9] and Brian et al. [10] were used to discriminate the vehicles of fire-retardant coatings. The results showed that seven out of ten types of fire-retardant coatings used polyvinyl acetate and acrylate as vehicle, two used alkyd resin, and only one used the synthetic resin developed by the manufacturer as the vehicle. In addition to FT-IR, SEM/EDS was used to perform elemental analysis to help further distinguish different types and brands of fire-retardant coatings. While the two types of intumescent fire-retardant coatings of brand B gave extremely similar IR spectra (Fig. 2) and were therefore indistinguishable, their EDS spectra were different as type B-2 contained sulfur but type B-1 does not and also type B-2 contained higher intensity ratio of  $\text{Ti/P}$  than that of type B-1 (Fig. 3).

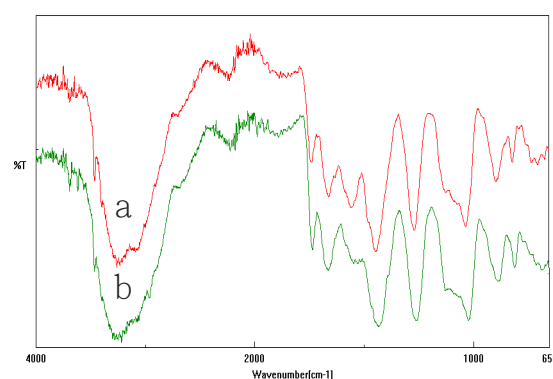


**Fig. 2** The IR absorption spectra of types B-1 (a) and B-2 (b).

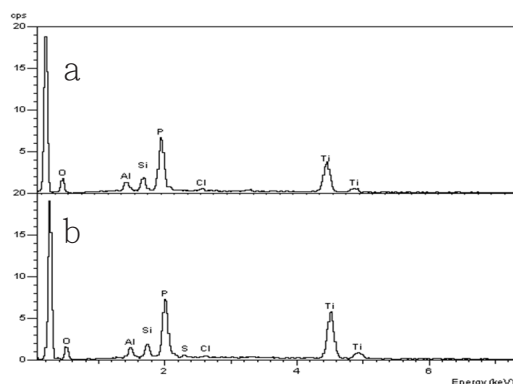


**Fig. 3** The EDS spectra of types B-1 (a) and B-2 (b).

### *Comparative analysis of fire-retardant coatings before and after combustion*

No matter how different were the pre-combustion IR spectra, different fire-retardant coatings had similar post-combustion (burned by CNS6532) IR absorption peaks as is shown in Fig. 4(c), indicating similar combustion products were formed. The major absorption peaks in Fig. 4(c) appeared at  $3261\text{ cm}^{-1}$ ,  $2360\text{ cm}^{-1}$ ,  $1635\text{ cm}^{-1}$ , and  $1428\text{ cm}^{-1}$ , along with a broader absorption band around  $1200\text{--}1000\text{ cm}^{-1}$ . The post-combustion absorption peak at  $3261\text{ cm}^{-1}$  decreased in intensity, while the peak at  $2360\text{ cm}^{-1}$  representing an O=P-OH group was more notable after combustion. The previous absorption peak at  $1732\text{ cm}^{-1}$  corresponding to a C=O group disappeared after combustion and a broad band at about  $1635\text{ cm}^{-1}$  appeared instead, suggesting the formation of an unsaturated char layer owing to dehydration during the combustion. The absorption peak at  $1428\text{ cm}^{-1}$  represented N-H and C-H groups. The peaks representing pentaerythritol in the foamer at  $1680\text{ cm}^{-1}$  and  $890\text{ cm}^{-1}$  attenuated or disappeared, implying the formation and evaporation of  $\text{NH}_3$  after combustion. That the previous absorption peak at  $1038\text{ cm}^{-1}$  representing a P-O-P group disappeared and that the broad absorption band emerged around  $1200\text{--}1000\text{ cm}^{-1}$  indicated that complex P-O-C were synthesized from phosphate and char former when heated. As to the EDS analysis Fig. 5 showed that the major elements, phosphorous (P) and titanium (Ti), in the coating were not affected by the combustion, and elements such as aluminum (Al), silicon (Si), and sodium (Na) were also retained after combustion. In addition, it

was found that all the volatile chlorine (Cl) and sulfur (S) in the fire-retardant coating disappeared after combustion

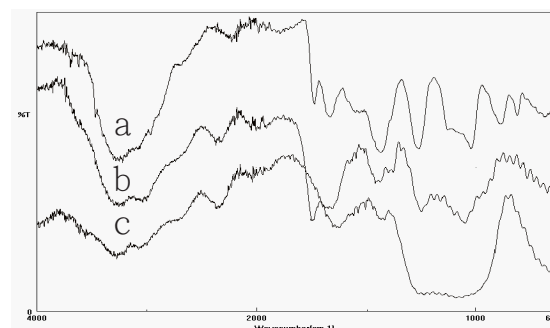


**Fig. 4** The IR spectra of fire-retardant coating, type B-2, before combustion (a), boundary layer after combustion (b), and char layer after combustion (c).

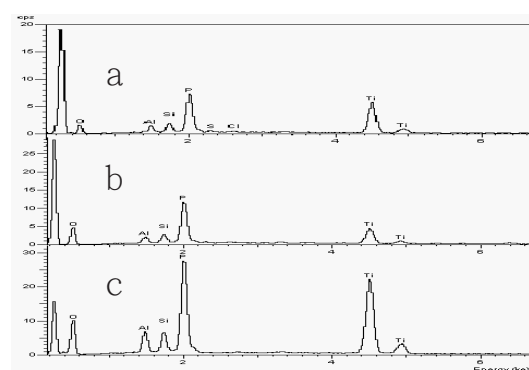


**Fig. 5** The EDS spectra of fire-retardant coating, type B-2, before combustion (a), boundary layer after combustion (b), and char layer after combustion (c).

### *Comparative analysis of mixed fire retardant-architectural coatings*

Although IR band intensity is not linearly proportional to analyte concentration and, hence, cannot be used for quantitative analysis, it still holds true that the stronger an IR band, the higher concentration of the analyte. At the volume ratio of 1:2, the mixed coating showed major IR absorption peaks that were similar to the band around  $1700\text{--}650\text{ cm}^{-1}$  in the spectra of common architectural coatings. The peak at  $1670\text{ cm}^{-1}$  was not present, and the peak at  $3200\text{ cm}^{-1}$  was significantly weaker than that at  $1735\text{ cm}^{-1}$ . At the

volume ratio of 1:1, the amplitude of the peak at  $1735\text{ cm}^{-1}$  was comparable to that of the broad band around  $3289\text{--}3278\text{ cm}^{-1}$ . An additional peak appeared at  $1665\text{ cm}^{-1}$ . The peak at  $1670\text{ cm}^{-1}$  in the spectra of common architectural coatings before mixing was stronger than that at  $1735\text{ cm}^{-1}$ . At the volume ratio of 1:1, the peak at  $1735\text{ cm}^{-1}$  was still weaker than that at  $1670\text{ cm}^{-1}$ . At the volume ratio of 2:1, the peak at  $1735\text{ cm}^{-1}$  was stronger than that at  $1670\text{ cm}^{-1}$ , indicating a lower content of P in the coating. In addition, a peak at around  $3200\text{ cm}^{-1}$  was stronger than the peak at  $1735\text{ cm}^{-1}$ . Thus, the mixing of a common architectural coating with a fire-retardant coating could be detected by comparing their absorption peak at  $1735\text{ cm}^{-1}$  with the peaks at  $3200\text{ cm}^{-1}$  and  $1680\text{ cm}^{-1}$ , respectively (Fig. 6).

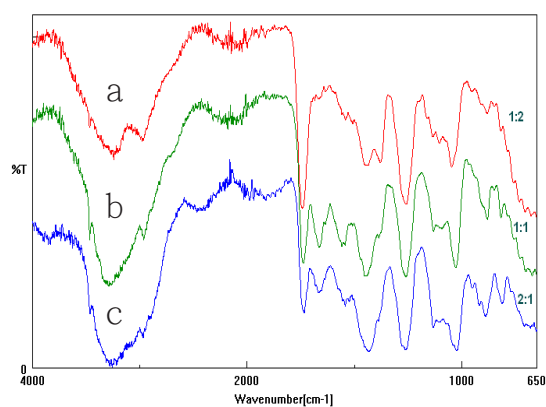


**Fig. 6** The pre-combustion IR absorption spectra of mixed fire retardant (type B-2)-architectural (type G-1) coating at volume mixing ratios of 1:2 (a), 1:1 (b), and 2:1(c).

The EDS analysis showed that the relative content of P for ammonium polyphosphate in a fire-retardant coating decreased after mixing with an architectural coating, while the relative content of Ti increased (Fig. 7). Since there were no P in common architecture paints, the change in contents of P and Ti could be used as an indicator of the mixing ratio. The counts of X-ray received every second (counts per second, CPS) in an EDS spectrum were used to determine the contents of P and Ti, and the index  $P/(P+Ti)$  was calculated to estimate the mixing ratio. Thus, a coating with  $P/(P+Ti)$  value greater than 0.46 was considered to be similar to fire-retardant coating, and that less than 0.14, similar to architectural paint (Table 3).

**Table 3** The  $P/(P+Ti)$  values calculated for various mixed fire retardant (type B-2)-architectural (type G) coating.

Mixing ratio of fire-retardant coating to architectural coating	$P/(P+Ti)^a$
0 : 1	0
1 : 2	0.14
1 : 1	0.35
2 : 1	0.46
1 : 0	0.56

<sup>a</sup> Each value shown herein represents the mean of two measurements.

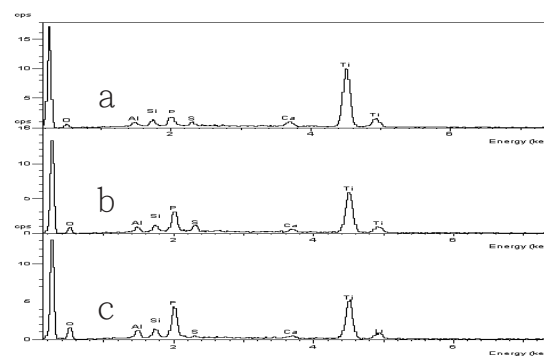


**Fig. 7** The pre-combustion EDS spectra of mixed fire retardant (type B-2)-architectural (type G-1) coatings at volume mixing ratios of 1:2 (a), 1:1 (b), and 2:1 (c).

### Forensics of mixed coatings after combustion

After the surface flammability test on mixed fire-retardant coatings in accordance with CNS6532, the uncoated plywood cracked severely. With the increasing ratio of fire-retardant coating to architectural coating, the intumescent effect became more evident and the cracking on the plywood surface became more unobvious. Specifically, the mixed fire retardant-architectural coating at the volume mixing ratio of 1:2 showed no apparent intumescence on the burnt surface. At the mixing ratio of 1:1, the coated surface displayed slight intumescence, but still cracked on the plywood surface. The intumescent effect on the coated surface became evident at the mixing ratio of 2:1, where only slight cracking appeared on the plywood surface. Thus, the surface flammability test enabled the identification of a mixed fire retardant-

architectural coating. Such immoral activities as using too little fire-retardant materials during coating will be revealed after fire accidents.

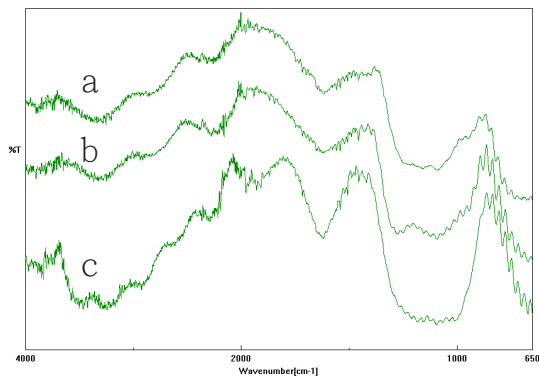


**Fig. 8** The post-combustion IR absorption spectra of mixed fire retardant (type B-2)-architectural (type G-1) coatings at volume mixing ratios of 1:2 (a), 1:1 (b), and 2:1 (c).

After combustion, there was no fundamental difference between the IR spectra of the mixed coating and the unmixed fire-retardant coating. Furthermore, the previous IR absorption peaks at  $1735\text{ cm}^{-1}$ ,  $1670\text{ cm}^{-1}$ ,  $1442\text{ cm}^{-1}$ , and  $1265\text{ cm}^{-1}$  all disappeared, and a broad absorption band at around  $1200\text{--}1000\text{ cm}^{-1}$  formed in the IR spectrum of the char layer (Fig. 8). It follows that EDS analysis might serve as a secondary discrimination (Fig. 9). Here, the calculated  $P/(P+Ti)$  value was used as the criteria for the identification of a mixed fire retardant-architectural coating. That is, the tested coating was determined to have been mixed with a common architecture coating if the  $P/(P+Ti)$  value was less than 0.46 (Table 3).

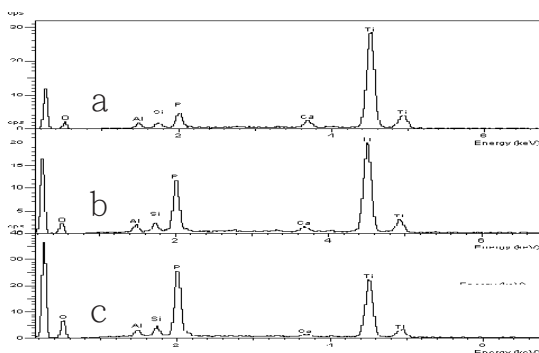


**Fig. 9** The post-combustion EDS spectra of mixed fire retardant (type B-2)-architectural (type G-1) coating at the volume mixing ratio of 1:2 (a), 1:1 (b), and 2:1 (c).

## Conclusions

Fire-retardant coatings of different brands vary from each other owing to differences in the vehicle, filler, and ratio of contents. Prior to combustion, they can be distinguished from each other by combined FTIR and SEM/EDS analyses on the coating film under normal temperatures. After combustion, however, the IR data of the char layers were all too similar to discriminate regardless of the brand and type. Fortunately, SEM/EDS enabled the detection of characteristic elements (except for volatile S and Cl) in the coatings, which provides a convenient way to discriminate between fire-retardant coatings of different brands and types.

The combination of FTIR and SEM/EDS analyses can be applied to mixed coatings to assess whether a fire-retardant coating has been mixed with the architectural coating. As a result, such immoral activities as using too little authentic fire-retardant materials can be effectively detected. These mixed fire-retardant coatings will show largely impaired intumescent effects after combustion. In addition, although their IR spectra are indistinguishable, EDS spectra can be used to calculate the  $P/(P+Ti)$  value in order to estimate the volume mixing ratio of the mixed coating. However, it is necessary to identify the type of architectural coating prior examination.

When inspecting interior decorative fire-retardant coatings in public places, only minute quantities of coating sample are required. They can be sampled from proper sites without hurting the apparent surface of the coating. Specifically, in the laboratory, the diamond compression cell requires only a trace amount of sample to run the FTIR analysis. Conclusive analysis of fire-retardant coatings along with valuable fire safety and forensic information can be achieved using combined micro-FTIR and SEM/EDS.

## References

1. Omrane A, Wang YC, Göransson U, Holmstedt G, Aldén. Intumescent coating surface temperature measurement in a cone calorimeter using laser-induced phosphorescence. *Fire Safety J* 2007; 42(1):68-74.
2. Wang Z, Hun E, Ke W. Effect of nanoparticles on the improvement in fire-resistant and anti-ageing properties of flame-retardant coating, *Surface &*

- Coating Technology, 2006; 200:5706-16.
3. Lv P, Wang Z, Hu K, Fan W. Flammability and thermal degradation of flame retarded polypropylene composites containing melamine phosphate and pentaerythritol derivative. *Polym Degrad Stab* 2005; 90(3):523-34.
  4. Wang Z, Han E, Ke W. Influence of expandable graphite on fire resistance and water resistance of flame-retardant coating. *Corros Sci* 2007; 49(5):2237-53.
  5. Scharf D, Nalepa R, Heflin R, Wusu T. Studies on flame retardant intumescent char: Part I. *Fire Safety J* 1992;19(1):103-17.
  6. Chinese National standards CNS6532 (1993) Method of test for incombustibility of internal finish material of building.
  7. Gu JW, Zhang GC, Dong SL, Zhang QY, Kong J. Study on preparation and fire-retardant mechanism analysis of intumescent flame-retardant coatings. *Surf Coat Technol* 2007; 201(18):7835-41.
  8. Wang Z, Han E, Ke W. Influence of nano-LDHs on char formation and fire-resistant properties of flame-retardant coating. *Prog Org Coat* 2005; 53(1)29-37.
  9. Saferstein R. *Forensic science hand book*. Englewood Cliffs, New Jersey: Prentice Hall, 1982.
  10. Caddy B. *Forensic examination of glass and paint, analysis and interpretation*. London: Taylor & Francis Ins, 2001.